

Remaining Useful Life Estimation of Aero-Engines with Self-Joint Prediction of Continuous and Discrete States

Rong-Jing Bao, Hai-Jun Rong, *Member, IEEE*, Zhi-Xin Yang, *Member, IEEE* and Badong Chen, *Senior Member, IEEE*

Abstract—The remaining useful life (RUL) estimation generally suffer from this problem of lacking prior knowledge to predefine the exact failure thresholds for machinery operating in dynamic environments. In this case, dynamic thresholds depicted by discrete states are effective to estimate the RUL of dynamic machinery. Currently, only few work considers the dynamic thresholds, and adopt different algorithms to predict the continuous and discrete states separately, which largely increases the complexity of the learning process. In this paper, we propose a novel prognostics approach for RUL estimation of aero-engines with self-joint prediction of continuous and discrete states within one learning framework. With modeling capability of self-adapting structure and parameters online, the quantized kernel recursive least squares (QKRLS) algorithm is introduced to predict the degrading states and also determine the discrete states with the kernel centers. The self-evolving dynamic kernel centers obtained during building predictors are automatically assigned as the discrete states for different engines without predefining them. Then, the RUL is estimated conveniently once the predicted degrading signals fall into the final fault state based on a distance metric. Finally, the results from turbofan engine datasets demonstrate the superiority of the proposed approach compared to other popular approaches.

Index Terms—Prognostics and health management (PHM), remaining useful life (RUL), aero-engines, quantized kernel recursive least squares (QKRLS).

I. INTRODUCTION

WITH the growing demand for improving the quality and reliability of aircrafts, prognostics and health management (PHM) has become one of the most important condition-based maintenance (CBM) activities in the aviation industries. The common thread among the various avenues of PHM technology development is the estimation of remaining useful life (RUL), which gives operators a potent tool in decision making by quantifying how much time is left until the functionality of a degrading component is lost. Accurate estimation of RUL plays an important role especially in aviation and aerospace systems such that the costs of excessive or insufficient maintenance may be avoided and fatal accidents may be

reduced. According to the researches and literatures, various prognostics approaches including model-based approaches, data-driven approaches and hybrid techniques combining them have been applied to RUL estimation [1]–[3]. The model-based approaches require a priori mathematical and physical knowledge of the process for constructing models. Nevertheless, it may be very difficult or even impossible to construct accurate physical models for real-world complex systems, which limits the applicability of model-based approaches.

In recent years, data-driven approaches have been a significant push towards prognostics due to their capability of predicting nonlinear functional and dynamic dependencies. It is feasible for data-driven approaches to automatically characterize and predict the behaviors of a component or system where the monitoring data can be easily observed by sensors to represent the fault propagation trends. Many data-driven approaches with emphasis on artificial intelligence (neural network, fuzzy system, genetic algorithm, etc.) and statistical learning (hidden Markov model, stochastic process, regression-based model, etc.) have been increasingly applied to the RUL estimation in different areas. Since the PHM challenge problem with turbofan engine degradation was published by the Prognostics CoE at NASA Ames Research Center in 2008 [4], more and more researchers around the world have devoted themselves to the development of prognostics, especially based on data-driven approaches.

As matters stand, the studies of data-driven approaches against this PHM challenge problem with turbofan engine degradation mostly concentrate on two ways. One way is to model the relationship between the sensor readings (or extracted features) and the RUL directly without considering the health states estimation. As early as 2008, recurrent neural networks (RNNs) are adopted to estimate the RUL directly without extracting underlying features that may appear in the data [5]. Recent researches have presented various approaches to estimate the RUL directly from the extracted features based on support vector regression [6] and deep convolutional neural network (CNN) [7]. Although these approaches neither need to estimate the health states nor need to predict the future failure progression, they require a significant amount of representative data and particularly generate black boxes that represent the relationship between the features and RUL. Thus, the degradation trend of an engine will be unknown, which makes it difficult for analysis in practical application.

In addition to the above-mentioned RUL estimation ap-

Rong-Jing Bao, Hai-Jun Rong are with the State Key Laboratory for Strength and Vibration of Mechanical Structures, Shaanxi Key Laboratory of Environment and Control for Flight Vehicle, School of Aerospace, Xi'an Jiaotong University, Xi'an 710049, China (e-mail: brj030@stu.xjtu.edu.cn, hjrong@mail.xjtu.edu.cn). Zhi-Xin Yang is with the Department of Electromechanical Engineering, Faculty of Science and Technology, University of Macau, Macao SAR 999078, China (e-mail: zxyang@umac.mo). Badong Chen is with the Institute of Artificial Intelligence and Robotics, School of Electronic and Information Engineering, Xi'an Jiaotong University, Xi'an 710049, China (e-mail: chenbd@mail.xjtu.edu.cn).

proaches, there also have been other attempts to depict the degradation patterns by building health indicator/index (HI) models. The HI is generally a curve that maps the current sensor readings or extracted features to the health patterns of an engine, wherein 1 denotes healthy and 0 denotes faulty. In some approaches, it is assumed to be a specific linear model [8] or an exponential model [9]. Furthermore, long short term memory based encoder-decoder (LSTM-ED) [10] and time series embeddings-based RNNs [11] are proposed to learn such mappings without making any assumption on the shape of HI model. Both of the two approaches have made improvements in the RUL estimation of aero-engines. However, the main challenge of these approaches is to find an appropriate mapping that can best explain the degradation behavior in the time series. The RUL estimation may fail if the matched patterns are unable to be found.

Another way of estimating the RUL is to determine the degradation through the continuous and discrete states. The continuous states represent the values of degrading signals while the discrete ones denote the fault modes. The utilization of discrete states provides the failure thresholds for continuous states of signals, which is able to reduce the uncertainty of RUL estimates. In [12], the discrete states are initially proposed by using an evidential Markovian classifier. In this approach, the discrete states are manually segmented into four states such that the discrete states of different engine units are all assumed to be the same. Further improved in [13], the joint prediction of continuous and discrete states, namely the evidential prognostics based on K-Nearest neighbors algorithm (EVIPO-KNN), is firstly proposed for PHM applications. However, in this approach the number of the discrete states is still assigned with fixed value rather than dynamic one for continuous observations. Actually, in practical applications, the behavior of the real aero-engines varies according to different initial conditions and operational environments. The pre-assumed fault modes are not suitable for all different operation conditions in which the degradation levels towards failure status are different accordingly.

This problem is addressed in [14], [15] where the summation wavelet-extreme learning machine (SW-ELM) algorithm is used to build prediction models and the subtractive-maximum entropy fuzzy clustering (S-MEFC) algorithm is applied to dynamically assign the fault modes where the cluster centers are equivalent to the fault modes. Although, the thresholds are dynamically determined without pre-assuming any failure thresholds in these two work, the state prediction and fault mode determination are obtained in an independent way through two different learning algorithms. Moreover, in [14] the univariate predictors are constructed to predict the continuous states. An aero-engine system generally contains multi-dimensional sensor measurements and thus the amount of the predictors is that of the sensors. In this case, the quantity of the constructed predictors may be very large for multiple learning instances with multi-dimensional measurements, which will increase the modeling burden. To solve this problem, the multivariate predictors are built in [15]. Besides, in the existing work [12]–[15], whatever the thresholds are fixed and dynamic, the thresholds assigned to the new test

instance are determined by considering the similarity distance among the known fault modes and the test instance.

In this paper, we propose a novel prognostics approach for RUL estimation of aero-engines with self-joint prediction of continuous and discrete states within one learning framework. To achieve this, the quantized kernel recursive least squares algorithm (QKRLS) [16] is adopted in our work. The QKRLS belongs to a class of nonlinear adaptive filtering algorithms derived in reproducing kernel Hilbert space (RKHS) based on the linear structure of this space. During the modeling process of the QKRLS, it adopts the self-evolving learning process [17], [18] to self-adapt both the structures and parameters online to capture the dynamical changes of data patterns. The structure of the QKRLS is related with the kernel centers and identified through an online vector quantization method. The kernel centers partition the input space into smaller regions. Similar to [14], [15], they can regarded as the fault modes. Considering these, the major contribution in this work are summarized as follows:

- (1) Unlike the existing work, the proposed approach only needs to build the predictors without requiring any classifiers or clusters to determine the degradation states. The established predictors have the capability of not only predicting the degrading states of the monitored aero-engines but also determining the discrete states dynamically. Each discrete state represents a degree of degradation during the running cycles of an aero-engine.
- (2) In this proposed approach, the established predictors are multivariate degradation-based prognostics models by considering all the sensor measurements together. This is different from some existing work where the univariate predictors are built by considering only one sensor measurement each time. Moreover, they have a higher level of flexibility and autonomy thanks to the ability to evolve their structure according to the coming data information and thus are very suitable to deal with data shift and drift due to changes in the operating environment over time suffered by the aero-engines.
- (3) Different from the existing work where only the distance criterion is applied to obtain the optimum predictors and failure thresholds for the testing instances, two matching criteria (i.e., the error criterion and the distance criterion) are used in our work such that each testing engine unit can obtain the optimum predictor to conduct the RUL estimation. This further increases the estimation accuracy.

The rest of this paper is organized as follows. Section II presents the proposed approach including predictor establishment and determination of discrete states using the QKRLS algorithm. In section III, we give the method of estimating the RUL during the self-prediction of continuous and discrete states. Performance evaluations are demonstrated for the proposed approach on the PHM2008 challenge dataset in section IV. Finally, we give the conclusion in section V.

II. SELF-JOINT PREDICTION OF CONTINUOUS AND DISCRETE STATES

The main idea of the proposed approach is to build multivariate degradation prognostics models, which are able to

achieve the continuous and discrete state prediction of aero-engines simultaneously. The continuous states represent the values of sensor measurements or features while the discrete ones denote the aero-engine health conditions during the degradation. In the following, their self-joint prediction is described in details.

A. Establishment of Predictors

For a training dataset \mathbf{T} given by (1), it contains multidimensional signals of s sensors and t_f running cycles in a time series.

$$\mathbf{T} = \begin{bmatrix} x_1^1 & \cdots & x_{t_f}^1 \\ \vdots & \ddots & \vdots \\ x_1^s & \cdots & x_{t_f}^s \end{bmatrix}_{s \times t_f} \quad (1)$$

For establishing a predictor, the training dataset \mathbf{T} is reorganized in the following form

$$\tilde{\mathbf{T}} = \{(\mathbf{x}_t, \mathbf{d}_t)\} \quad (2)$$

where $\mathbf{x}_t = [x_{t-k}^1, \dots, x_{t-1}^1, \dots, x_{t-k}^s, \dots, x_{t-1}^s]^T$ is an $(s \cdot k) \times 1$ dimensional input of the predictor, $\mathbf{d}_t = [x_t^1, \dots, x_t^s]^T$ is an $s \times 1$ dimensional output of the predictor and k is the number of regressors. The modeling of the predictor for continuous states is established as follows:

$$\hat{\mathbf{d}}_t = P(\mathbf{x}_t, \hat{\beta}_t, \mathbf{C}_t) \quad (3)$$

where P denotes a nonlinear mapping function, $\hat{\beta}_t$ and \mathbf{C}_t are respectively the weight parameter and quantization codebook existing in the QKRLS algorithm. The modeling of the multi-input and multi-output (MIMO) predictor using the QKRLS algorithm is shown in Fig. 1.

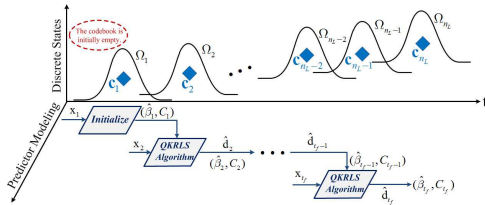


Fig. 1: Modeling of predictor $P(\mathbf{x}, \hat{\beta}, \mathbf{C})$ with QKRLS algorithm.

In the QKRLS algorithm, the learning problem of a continuous mapping $P : \mathbb{X} \rightarrow \mathbb{R}$ is regarded as a least squares regression based on a sequence of the observed dataset $\{(\mathbf{x}_t, \mathbf{d}_t) | t = 1, \dots, t_f\}$, where $\mathbb{X} \subset \mathbb{R}$ is the input space. According to the Mercer's theorem, any Mercer kernel $\kappa(\cdot, \cdot)$ is able to transform the input space \mathbb{X} to an infinite dimensional reproducing kernel Hilbert space \mathbb{F}_κ (RKHS) by means of a nonlinear mapping ϕ , i.e., $\kappa(\mathbf{x}, \mathbf{x}') = \langle \phi(\mathbf{x}), \phi(\mathbf{x}') \rangle_{\mathbb{F}_\kappa}$. In the feature space the inner product $\langle \cdot, \cdot \rangle_{\mathbb{F}_\kappa}$ can be easily computed using the well known kernel trick $\kappa(\mathbf{x}, \mathbf{x}') = \phi(\mathbf{x})^T \phi(\mathbf{x}')$. In this paper, the commonly used Gaussian kernel with kernel width σ is selected as the Mercer kernel [16].

To achieve the mapping P associated with $\hat{\beta}$, one needs to find such a high-dimensional weight $\hat{\mathbf{B}} \in \mathbb{F}_\kappa$ in the feature space \mathbb{F}_κ for the learning problem which minimizes

$$\min_{\mathbf{B} \in \mathbb{F}_\kappa} \alpha \|\mathbf{B}\|_{\mathbb{F}_\kappa}^2 + \sum_{t=1}^{t_f} \|\mathbf{d}_t - \mathbf{B}^T \phi(Q(\mathbf{x}_t))\|^2 \quad (4)$$

where α is the regularization factor that controls the smoothness of the solution and avoids over-fitting. The feature space \mathbb{F}_κ is isometric-isomorphic to the RKHS induced by the kernel. The relationship between $\hat{\mathbf{B}}$ and $\hat{\beta}$ can be easily recognized by the following expression

$$\hat{\mathbf{B}} = \Phi \hat{\beta} \quad (5)$$

where $\Phi = [\phi(\mathbf{x}_1), \phi(\mathbf{x}_2), \dots, \phi(\mathbf{x}_{t_f})]$, $Q(\cdot)$ denotes a vector quantizer (VQ). As shown in Fig. 1, the quantization codebook \mathbf{C} is initially empty and is assumed that it contains n_L code vectors at $t = t_f$, i.e., $\mathbf{C}_{t_f} = \{c_n \in \mathbb{X} | n \in \mathcal{L}\}$, where $\mathcal{L} = \{1, 2, \dots, n_L\}$ is the index set that contains n_L elements. And consequently, the vector quantization operator $Q(\mathbf{x}_t)$ maps the input $\{\mathbf{x}_t | t = 1, \dots, t_f\}$ in \mathbb{X} into one of the n_L code vectors in the quantization codebook \mathbf{C}_{t_f} . By partitioning the input space \mathbb{X} into n_L disjoint and exhaustive regions $\Omega_1, \Omega_2, \dots, \Omega_{n_L}$, where we define $\Omega_n = Q^{-1}(c_n) \in \mathbb{X}$. The values of the code vectors specify the vector quantization operator $Q(\mathbf{x}_t)$, i.e., $Q(\mathbf{x}_t) = c_n$, if $\mathbf{x}_t \in \Omega_n$. Defining M_n is the number of the input data that lies in the n th region Ω_n , we have

$$M_n = |\{\mathbf{x}_t | \mathbf{x}_t \in \Omega_n, 1 \leq t \leq t_f\}| \quad (6)$$

$|Z| \geq 0$ denotes the cardinality of a set Z and $\sum_{n=1}^{n_L} M_n = t_f$. Define $\mathbf{d}_{n,i}$ as the desired output that corresponds to the i th element from the n th region, we have $\mathbf{d}_{n,i} = \mathbf{d}_t$ when $\mathbf{x}_t \in \Omega_n$ and $|\{\mathbf{x}_{t'} | \mathbf{x}_{t'} \in \Omega_n, 1 \leq t' \leq t\}| = i$. Then (4) can be rewritten as follows

$$\min_{\mathbf{B} \in \mathbb{F}_\kappa} \alpha \|\mathbf{B}\|_{\mathbb{F}_\kappa}^2 + \sum_{n \in \mathcal{L}} \left(\sum_{i=1}^{M_n} \|\mathbf{d}_{n,i} - \mathbf{B}^T \phi(c_n)\|^2 \right) \quad (7)$$

Consequently, the solution to (7) can be derived as follows

$$\hat{\mathbf{B}} = \Phi (\Lambda \Phi^T \Phi + \alpha \mathbf{I})^{-1} \bar{\mathbf{d}} \quad (8)$$

where $\Phi = [\phi(c_1), \phi(c_2), \dots, \phi(c_{n_L})]$, $\Lambda = \text{diag}[M_1, M_2, \dots, M_{n_L}]$ and

$$\bar{\mathbf{d}} = [\sum_{i=1}^{M_1} \mathbf{d}_{1,i}, \sum_{i=1}^{M_2} \mathbf{d}_{2,i}, \dots, \sum_{i=1}^{M_{n_L}} \mathbf{d}_{n_L,i}]^T \quad (9)$$

According to (5) and (8), we can obtain

$$\hat{\beta} = (\Lambda \Phi^T \Phi + \alpha \mathbf{I})^{-1} \bar{\mathbf{d}} = (\Lambda \Psi + \alpha \mathbf{I})^{-1} \bar{\mathbf{d}} \quad (10)$$

where $\Psi = \Phi^T \Phi$ is the Gram matrix and its elements are $\Psi_{ij} = \kappa(c_i, c_j)$.

When a predictor $P(\hat{\beta}, \mathbf{C})$ of (3) is established, the codebook $\mathbf{C} = \{c_n | n = 1, 2, \dots, n_L\}$ is obtained accordingly. The multivariate degrading signals of the training dataset $\{\mathbf{x}_t | \mathbf{x}_t \in \mathbb{R}^{s \cdot k}, t = 1, \dots, t_f\}$ can be partitioned into n_L regions, where \mathbf{x}_t belongs to the n th region Ω_n by calculating

$$n = \arg \min_{1 \leq n \leq n_L} \|\mathbf{x}_t - c_n\| \quad (11)$$

Each region Ω_n corresponds to a code vector \mathbf{c}_n as its center and is considered as a discrete state of an engine. The first region Ω_1 indicates the initial state where the engine starts. Relatively, the final region Ω_{n_L} represents the failure state where the engine comes to end-of-life (EoL). It should be noted that all the regions can be viewed as the transition from normal states to degrading states until the final fault state. Thus, the discrete states are equivalent to the codebook \mathbf{C} . When the codebook \mathbf{C} is obtained, the discrete states representing the failure thresholds are determined. The following describes the details about determining the discrete states.

B. Determination of Discrete States

By employing an online VQ method [16], [19], the codebook is built and the code vectors to the data are assigned automatically from the specific training dataset $\{(\mathbf{x}_t, \mathbf{d}_t) | t = 1, \dots, t_f\}$. Initially the first data sample is chosen as its first code vector, that is $\mathbf{c}_1 = \mathbf{x}_1$. When more data samples arrive, the code vectors are formed based on the distance evaluation between the new data \mathbf{x}_{t+1} and the existing code vectors. Two cases are considered in the following to derive the codebook \mathbf{C}_t for determining the discrete states along with updating the weight parameter $\hat{\beta}$ in (10). In the following, we denote

$$\mathbf{A}_t = (\Lambda_t \Psi_t + \alpha \mathbf{I})^{-1} \quad (12)$$

and (10) becomes $\hat{\beta}_t = \mathbf{A}_t \bar{\mathbf{d}}_t$.

Case 1: $\|\mathbf{x}_{t+1} - \mathbf{C}_{t,i}\|_{i=1}^{|C_t|} \leq \varepsilon$, ε is the quantization size.

Under this circumstance, the new data \mathbf{x}_{t+1} is close enough to all the existing code vectors and thus the codebook remains unchanged $\mathbf{C}_{t+1} = \mathbf{C}_t$. We have

$$\Phi_{t+1} = \Phi_t = [\phi(\mathbf{c}_1), \phi(\mathbf{c}_2), \dots, \phi(\mathbf{c}_{n_{|C_t|}})] \quad (13)$$

$$\Psi_{t+1} = \Phi_{t+1}^T \Phi_{t+1} \quad (14)$$

The input \mathbf{x}_{t+1} is quantized to the i^* th element of the codebook \mathbf{C}_t defined as \mathbf{C}_{t,i^*} . i^* is computed as follows

$$i^* = \arg \min_{1 \leq i \leq |C_t|} \|\mathbf{x}_{t+1} - \mathbf{C}_{t,i}\| \quad (15)$$

The matrix Λ_{t+1} and \mathbf{A}_{t+1} are updated as follows

$$\Lambda_{t+1} = \Lambda_t + \omega_t \omega_t^T \quad (16)$$

$$\mathbf{A}_{t+1} = [\mathbf{A}_t^{-1} + \omega_t \omega_t^T \Psi_t]^{-1} \quad (17)$$

where $\omega_t = [\omega_1, \omega_2, \dots, \omega_{|C_t|}]^T$, the i^* th element of ω is 1 while other elements are all 0. By using the matrix inversion lemma [20], we derive

$$\mathbf{A}_{t+1} = \mathbf{A}_t - \frac{\mathbf{A}_{t,i^*} [\Psi_{t,i^*}^T \mathbf{A}_t]}{1 + \Psi_{t,i^*}^T \mathbf{A}_{t,i^*}} \quad (18)$$

where \mathbf{A}_{t,i^*} and Ψ_{t,i^*} represent the i^* th columns of the matrices \mathbf{A}_t and Ψ_t respectively. Then $\hat{\beta}_{t+1}$ can be updated as follows

$$\hat{\beta}_{t+1} = \mathbf{A}_{t+1} \bar{\mathbf{d}}_{t+1} = \hat{\beta}_t + \frac{\mathbf{A}_{t,i^*} [\mathbf{d}_{t+1} - \Psi_{t,i^*}^T \hat{\beta}_t]}{1 + \Psi_{t,i^*}^T \mathbf{A}_{t,i^*}} \quad (19)$$

Case 2: $\|\mathbf{x}_{t+1} - \mathbf{C}_{t,i}\|_{i=1}^{|C_t|} > \varepsilon$

Under this circumstance, the new data \mathbf{x}_{t+1} is sufficiently far from all the existing code vectors and represents a new operating regime. Then, the codebook is updated $\mathbf{C}_{t+1} = \{\mathbf{C}_t, \mathbf{x}_{t+1}\}$ by accepting the new data as a new code vector. We have $\Phi_{t+1} = [\Phi_t, \phi(\mathbf{x}_{t+1})]$. The matrix Λ_{t+1} and \mathbf{A}_{t+1} are updated as follows

$$\Lambda_{t+1} = \begin{bmatrix} \Lambda_t & \\ & 1 \end{bmatrix} \quad (20)$$

$$\mathbf{A}_{t+1} = \begin{bmatrix} \mathbf{A}_t^{-1} & \Lambda_t \mathbf{h}_{t+1} \\ \mathbf{h}_{t+1}^T & \alpha + \kappa(\mathbf{x}_{t+1}, \mathbf{x}_{t+1}) \end{bmatrix}^{-1} \quad (21)$$

where the kernel matrix in (21) can be rewritten as

$$\mathbf{h}_{t+1} = [\kappa(\mathbf{C}_{t,1}, \mathbf{x}_{t+1}), \kappa(\mathbf{C}_{t,2}, \mathbf{x}_{t+1}), \dots, \kappa(\mathbf{C}_{t,|C_t|}, \mathbf{x}_{t+1})]^T \quad (22)$$

By using the block matrix inversion identity [20], we have

$$\mathbf{A}_{t+1} = r_{t+1}^{-1} \begin{bmatrix} \mathbf{A}_t r_{t+1} + \bar{\mathbf{q}}_{t+1} \mathbf{q}_{t+1}^T & -\bar{\mathbf{q}}_{t+1} \\ -\mathbf{q}_{t+1}^T & 1 \end{bmatrix} \quad (23)$$

where $r_{t+1} = \alpha + \kappa(\mathbf{x}_{t+1}, \mathbf{x}_{t+1}) - \mathbf{h}_{t+1}^T \bar{\mathbf{q}}_{t+1}$, $\bar{\mathbf{q}}_{t+1} = \mathbf{A}_t \Lambda_t \mathbf{h}_{t+1}$, $\mathbf{q}_{t+1} = \mathbf{A}_t^T \mathbf{h}_{t+1}$.

Then $\hat{\beta}_{t+1}$ can be updated as follows

$$\hat{\beta}_{t+1} = \mathbf{A}_{t+1} \bar{\mathbf{d}}_{t+1} = \begin{bmatrix} \hat{\beta}_t - \mathbf{q}_{t+1} r_{t+1}^{-1} \mathbf{e}_{t+1} \\ r_{t+1}^{-1} \mathbf{e}_{t+1} \end{bmatrix} \quad (24)$$

where $\mathbf{e}_{t+1} = \mathbf{d}_{t+1} - \mathbf{h}_{t+1}^T \hat{\beta}_t$ is the error between the desired output and the estimated output of the predictor. Ultimately, we have obtained the self-joint prediction of continuous and discrete states by using the QKRLS algorithm, which is summarized concisely in Algorithm 1.

Algorithm 1 self-prediction of continuous and discrete states with QKRLS algorithm

Sample: $\{(\mathbf{x}_t, \mathbf{d}_t) | t = 1, \dots, t_f\}$

Initialization: Initialize $\mathbf{C}_1 = \{\mathbf{c}_1 = \mathbf{x}_1\}$, $\Lambda_1 = [1]$, $\mathbf{A}_1 = [\kappa(\mathbf{c}_1, \mathbf{c}_1) + \alpha]^{-1}$, $\hat{\beta}_1 = \mathbf{A}_1 \mathbf{d}_1$, and choose a proper quantization size ε and a proper regularization parameter α .

Calculation: For $(\mathbf{x}_{t+1}, \mathbf{d}_{t+1})$

if $\|\mathbf{x}_{t+1} - \mathbf{C}_{t,i}\|_{i=1}^{|C_t|} \leq \varepsilon$ **then**

 Keep the codebook unchanged: $\mathbf{C}_{t+1} = \mathbf{C}_t$; Calculate i^* using (15); update the matrix Λ_{t+1} using (16); update \mathbf{A}_{t+1} using (18).

 Predict $\bar{\mathbf{d}}_{t+1} = \Psi_{t,i^*}^T \hat{\beta}_t$.

 Update the weight parameter $\hat{\beta}_{t+1}$ using (19).

else

 Update the codebook $\mathbf{C}_{t+1} = \{\mathbf{C}_t, \mathbf{x}_{t+1}\}$; update the matrix Λ_{t+1} using Eq. (20); update \mathbf{h}_{t+1} using (22); update \mathbf{A}_{t+1} using (23).

 Predict $\hat{\mathbf{d}}_{t+1} = \mathbf{h}_{t+1}^T \hat{\beta}_t$.

 Update the weight parameter $\hat{\beta}_{t+1}$ using (24).

end if

Predictor: Obtain $P(\hat{\beta}, \mathbf{C})$.

After the predictors and the discrete states are constructed based on the training dataset of engines, the RUL is further estimated. This is depicted below.

III. RUL ESTIMATION

For a testing dataset \mathcal{S} given by

$$\mathcal{S} = \begin{bmatrix} \tilde{x}_1^1 & \cdots & \tilde{x}_{t_c}^1 \\ \vdots & \ddots & \vdots \\ \tilde{x}_1^s & \cdots & \tilde{x}_{t_c}^s \end{bmatrix}_{s \times t_c} \quad (25)$$

the multidimensional signals are observed by s sensors when an engine operates normally up to t_c running cycles before system failure. By reorganizing the testing dataset \mathcal{S} as well as (2) in the following form

$$\tilde{\mathcal{S}} = \{(\tilde{\mathbf{x}}_t, \mathbf{d}_t)\} \quad (26)$$

where $\tilde{\mathbf{x}}_t = [\tilde{x}_{t-k}^1, \dots, \tilde{x}_{t-1}^1, \dots, \tilde{x}_{t-k}^s, \dots, \tilde{x}_{t-1}^s]^T$ and $\mathbf{d}_t = [\tilde{x}_t^1, \dots, \tilde{x}_t^s]^T$.

Prior to the RUL estimation of a testing engine, its future degrading signals $\{\hat{\mathbf{d}}_t | t > t_c\}$ can be estimated by the predictor

$$\hat{\mathbf{d}}_t = P(\hat{\beta}, \mathcal{C}, \tilde{\mathbf{x}}_t) = [\hat{x}_t^1, \dots, \hat{x}_t^s]^T \quad (27)$$

where $t = t_c + 1, t_c + 2, \dots$. It can be seen that the prediction starts from $t = t_c + 1$ to predict the future degrading signals $[\hat{x}_{t_c+1}^1, \dots, \hat{x}_{t_c+1}^s]^T$ in time sequence. Particularly, when the time sequence $t \in [t_c + 2, t_c + k]$, the inputs contain the observed data \tilde{x}_t^i and the estimated data \hat{x}_t^i . And when the time sequence $t > t_c + k + 1$, the future degrading signals are all predicted by the estimated ones \hat{x}_t^i . The continuous prediction with multisteps-ahead for future degrading signals is shown in Fig. 2.

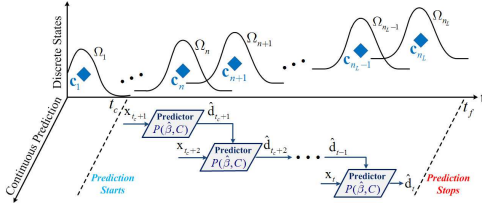


Fig. 2: Continuous state prediction with multisteps-ahead for future degrading signals.

For testing samples comprised of \mathfrak{N} time series, each time series is also from a different testing engine of the same fleet which has a diverse initial condition and operational environment. we need to determinate the optimum predictor for each time series such that an accurate RUL estimation can be obtained. For this purpose, two criteria are adopted here. The first one is named as the RMSE (Root Mean Square Error) criterion which is utilized to determinate the predictor for each specific testing dataset. It guarantees that the future degrading signals can be predicted precisely. Based on the RMSE criterion, appropriate predictors are determined through calculating the testing RMSE which is given as follows

$$\text{RMSE}_i = \sqrt{\sum_{t=1}^{t_c} \|\mathbf{d}_t - \hat{\mathbf{d}}_t\|^2}, i = 1, \dots, \mathfrak{M} \quad (28)$$

where $t \leq t_c$, \mathbf{d}_t is the desired output, $\hat{\mathbf{d}}_t = P^i(\hat{\beta}^i, \mathcal{C}^i, \tilde{\mathbf{x}}_t)$ is the output of the predictor, $\hat{\beta}^i$ and \mathcal{C}^i are the weight

parameter and codebook of the predictor P^i respectively. After \mathfrak{M} predictors are tested for a specific testing dataset $\tilde{\mathcal{S}}$, one can obtain the testing accuracies in ascending order as follows

$$\text{RMSE}_1 \leq \dots \leq \text{RMSE}_J \leq \dots \leq \text{RMSE}_{\mathfrak{M}} \quad (29)$$

According to the testing errors, the first J predictors with smaller errors $\{P^j | j = 1, \dots, J < \mathfrak{M}\}$ are selected under the RMSE criterion.

As mentioned above, each testing engine starts with a diverse initial condition such that the degrading process of each testing engine would be various. The degradation states of a testing engine represented by the discrete states are associated with the codebook \mathcal{C}^i of the predictor P^i . Therefore, the second criterion is based on a distance criterion, which is used to enhance the results determined by the RMSE criterion. Among J different type of discrete states obtained from predictors $\{P^1, P^2, \dots, P^J\}$, the suitable discrete states for $\tilde{\mathcal{S}}$ can be found by looking at the minimum Euclidean distance (ED) measurement

$$j^* = \arg \min_{1 \leq j \leq J} \sum_{n=1}^{n_L} \sum_{m=1}^{M_n} \|\tilde{\mathbf{x}}_m - \mathbf{c}_n^j\| \quad (30)$$

where M_n is the number of the input data $\tilde{\mathbf{x}}$ that lies in the n th region Ω_n , i.e., $\{\tilde{\mathbf{x}}_m | \tilde{\mathbf{x}}_m \in \Omega_n, 1 \leq m \leq M_n\}$, \mathbf{c}_n^j is the code vector of the j th predictor P^j , and $\sum_{n=1}^{n_L} M_n = t_c$. (28) and (30) are denoted as the self-determination criteria, under which each testing dataset $\{\tilde{\mathcal{S}}^n\}_{n \in \mathcal{L}1}$ is matched to its optimum predictor $\{P^{j^*}\}_{j^* \in \mathcal{L}2}$, and is represented as follows

$$\tilde{\mathcal{S}}^n \Rightarrow P^{j^*} \quad (31)$$

where $\mathcal{L}1 = \{1, \dots, \mathfrak{N}\}$ is the index set of testing engines that contains \mathfrak{N} time series and $\mathcal{L}2 = \{1, \dots, \mathfrak{M}\}$ is the index set of training engines that contains \mathfrak{M} time series.

Generally, when an engine fails to run or arrives at the fault mode at the failure time t_f , the degrading signals grow to the damage level. For a testing engine running up to the current time t_c before system failure, its health states of future degradation are unknown to the users. If the testing engine continues to operate and is degrading increasingly due to some wear and tear, the states of degradation will terminate at the fault state Ω_{n_L} . The discrete states are considered as different degrading levels of the degradation process.

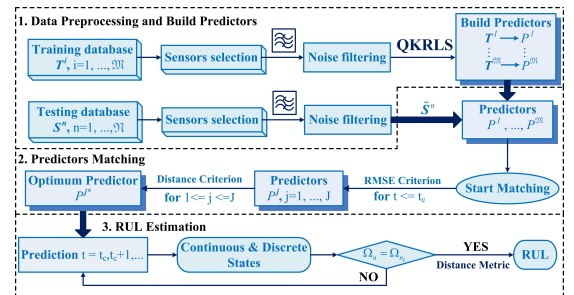


Fig. 3: Diagram of the proposed prognostics approach for RUL estimation.

In this study, the discrete states are determined during the predicting process simultaneously and directly rather than by

using the classifiers or clusters. The codebook of a predictor represents the states of an engine from healthy condition to fault mode, which is decided and computed through a vector quantizer. While the future degrading signals of a testing engine are predicted with its optimum predictor P^{j*} , the discrete states can be determined accordingly by the codebook C^{j*} of P^{j*} . If the predicted multidimensional signals $\tilde{\mathbf{x}}_t$ belong to the final region Ω_{n_L} of P^{j*} , the prediction of the testing engine stops. Once the predicted multidimensional signals $\tilde{\mathbf{x}}_t$ come into the final region Ω_{n_L} , the failure time t_f of this testing engine can be calculated by using the following distance metric

$$t_f = \min \left(\arg \min_{s.t. t > t_c} \|\tilde{\mathbf{x}}_t - \mathbf{c}_{n_L}\| \right) \quad (32)$$

And the RUL of this testing engine is estimated conveniently between the current time t_c and the failure time t_f

$$\hat{t}_{RUL} = t_f - t_c \quad (33)$$

The prediction of an aero-engine degradation and its RUL estimation is shown in Fig. 3. Based on the proposed prognostics approach, continuous state prediction and discrete state determination can be obtained simultaneously. The RUL of the testing engine is computed conveniently according to (32) and (33).

IV. APPLICATION AND RESULTS

A. Datasets, Parameters Setting and Evaluation Metrics

In order to demonstrate the performance of the proposed prognostics approach, three text files “train-FD001.txt”, “test-FD001.txt” and “RUL_FD001.txt” of the PHM 2008 challenge datasets [4] are employed here, wherein one condition and one fault mode are considered. In this paper, five predictable sensors [2, 8, 11, 13, 15] (7th, 13th, 16th, 18th and 20th column of the dataset) are employed for RUL estimation by a data-mining technique [15].

Prior to estimating the RUL, the sensor measurements are denoised by using the locally weighted scatter plot smoothing (LOWESS) algorithm with the span parameter setting to 10.5. Then, the denoised sensor measurements of the training dataset are normalized in the range $[0, 1]$ as well as the ones of the testing dataset. The number of regressors k is set to 3, J is set to 5. It should be noted that in this study all the established predictors of 100 training engine units use the same parameters $\sigma = 2$, $\varepsilon = 0.1$, $\alpha = 0.001$.

As in [6], [8]–[11], [13], [15], the following evaluation metrics are used for PHM performance evaluation such as coefficient of determination (R2), RUL Error PDF, mean square error (MSE), mean absolute error (MAE), mean absolute percentage error (MAPE) Score, Accuracy Rate. Their details can be referred to the above references.

B. Simulation Results and Comparison

1) *Analysis on an Engine Case*: Here the testing engine #17 is considered as an example, which operates normally to $t_c = 165$ running cycles. As shown in Table I, five predictors (P^9 , P^{51} , P^{59} , P^{29} and P^{28}) are selected based on the

RMSE criterion. Besides, the optimum predictor P^{51} with 86 discrete states can be obtained under the distance criterion by looking at the minimum Euclidean distance among these five predictors. It can be seen that the testing accuracy is within 0.01, which guarantees the good performance of continuous state prediction.

TABLE I: OPTIMUM PREDICTOR CHOSEN FOR TESTING ENGINE #17

RMSE	Distance(ED)	Predictor	Number of Discrete States
0.0089	16.318	51	86
0.0086	16.825	9	84
0.0093	16.837	28	79
0.0092	18.858	29	77
0.0092	19.162	59	104

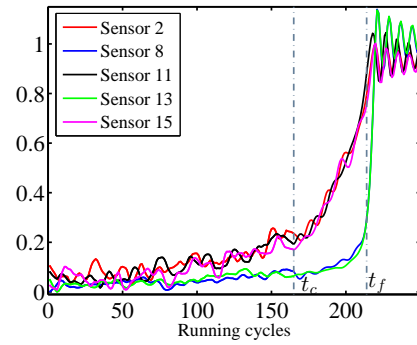


Fig. 4: Continuous state prediction of multidimensional future signals of the testing engine #17 ($S^{17} \Rightarrow P^{51}, t_c = 165, n_L = 86$).

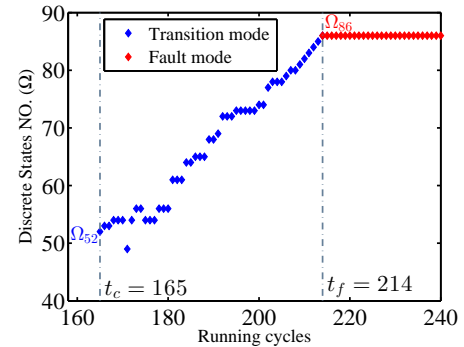


Fig. 5: Discrete states of the testing engine #17 along with the continuous prediction. The transition mode denotes only degrading states or a transition from normal to degrading states here.

The continuous prediction for multidimensional future signals of the testing engine #17 is shown in Fig. 4. Its future degrading signals ($t > t_c$) are all predicted by its optimum predictor P^{51} . From Fig. 4, it can be found that if the testing engine continues running after the failure time t_f , it will degrade heavily. Additionally, when the testing engine fails to run or is in a fault mode, the degrading signals grow to the damage level. In order to prevent the engine from running into the fault mode, the prediction of continuous and

TABLE II: COMPARISON RESULTS BETWEEN DIFFERENT APPROACHES FOR 100 TESTING ENGINES

Results\Approach	EVIPO-KNN [13]	IBL [8]	RULCLIPPER [9]	SWELM-SMEFC [15]	LR-ED ₂ [10]	SVR [6]	Embed-LR ₁ [11]	Self-Prediciton (Proposed)
R2	/	/	/	0.614	/	/	/	0.911
RUL Error PDF	[-85,120]	/	/	[-39,60]	/	/	/	[-53,43]
In time	53	54	67	48	67	70	59	78
Early (FN)	36	18	44	40	13	/	14	16
Late (FP)	11	28	56	12	20	/	27	6
MSE	/	/	176	/	164	/	155	153.7
MAE	/	/	10	/	9.9	/	9.8	7.34
MAPE	/	/	20%	/	18%	/	19%	9.95%
Score	/	/	216	1046	256	448.7	219	351.6
Accuracy Rate	53%	54%	67%	48%	67%	70%	59%	78%

discrete states proceeds simultaneously. During the process of predicting continuous states, each predicted multidimensional signal belongs to a specific discrete state Ω by computing (11). Thus, the prediction of continuous states stops by judging whether a predicted multidimensional signal enters into the final discrete state, i.e., the failure state Ω_{n_L} . And the failure time t_f and RUL of the testing engine is correspondingly estimated with (32) and (33). To illustrate these, Fig. 5 shows the predicted multidimensional signals associated with their discrete states between $[t_c, t_f]$ running cycles, wherein the fault grows increasingly until failure occurs. From Fig. 5, it can be seen that the testing engine #17 starts from state Ω_{52} corresponding with the current time $t_c = 165$ and terminates at state Ω_{86} corresponding with the failure time $t_f = 214$. Within $[165, 214]$ running cycles, the testing engine can be considered as in the transition mode which includes only degrading or from normal to degrading. For different testing engines, the discrete states may represent various conditions. Moreover, if the continuous prediction carries on after the failure time $t_f = 214$, all the predicted multidimensional signals will belong to the final state Ω_{86} and the testing engine will stuck in the fault mode. Therefore, it is demonstrated that the estimation of the failure time is reasonable and the testing engine can achieve a just-in-time prediction with the proposed approach.

2) *Results of 100 Testing Engine Units:* When 100 predictors $\{P^j(\hat{\beta}, C)|j = 1, \dots, 100\}$ are established based on the training dataset, 100 codebooks can be obtained accordingly. In each codebook, the code vectors are assigned dynamically and automatically by using the QKRLS algorithm. And the cardinality of the codebook is not only the number of the code vectors but also the number of the discrete states. After the optimum predictor for each testing engine is determined under the RMSE and distance criteria, the discrete states for every testing engine unit are obtained as well, which are shown in Fig. 6. From Fig. 6, it is obvious to find that the number of the discrete states varies from one testing engine unit to another. The dynamic discrete states also give a reasonable interpretation that the engines of the same fleet have various degree of wear and tear due to different initial conditions and operational environments.

For 100 testing engines matched to their optimal predictors P^{j*} , their remaining useful lives (RULs) can be estimated by using the distance metric associated with the final discrete state of the matched predictor P^{j*} respectively. The estimated RULs of 100 testing engines are shown in Fig. 7, from which

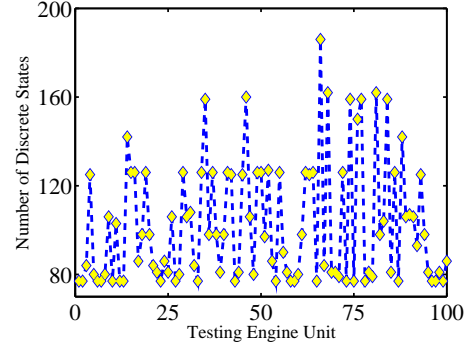


Fig. 6: Diversification of the discrete states for 100 testing engines (from #1 to #100) according to their own optimum predictor P^{j*} .

one can see that the estimated RULs are very close to the actual RULs. This demonstrates the robust performance of the proposed prognostics approach for estimating the RULs of the testing engine units without any prior knowledge about their real RULs and variability.

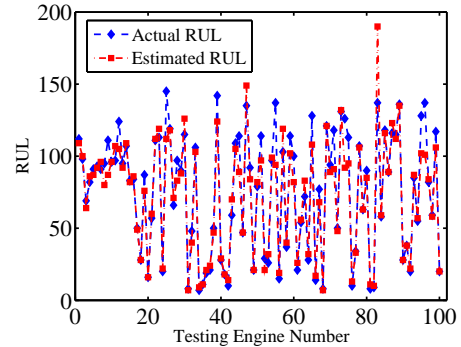


Fig. 7: Estimated RULs versus actual RULs of 100 testing engines.

3) *Comparison With Other Approaches:* Finally, we give the results of the RUL estimation for total 100 testing engines, which are summarized in Table II. The results are also compared to other popular prognostics approaches, such as EVIPO-KNN [13], IBL [8], RULCLIPPER [9], SWELM-SMEFC [15], LR-ED₂ [7], SVR [6] and Embed-LR₁ [11]. The results of these references are arranged in ascending order of the published year and are selected according to their best performances. Compared to SWELM-SMEFC, the

coefficient of determination R^2 we obtained is larger. Although the larger value of R^2 stands for better prediction, it is primarily designed for model selection using the training dataset. Thus, we suggest avoiding the use of this metric as a main tool for performance evaluations. The RUL error distribution of the proposed approach has the lower span $I = [-53, 43]$ than EVIPO-KNN and is similar with SWELM-SMEFC $I = [-39, 60]$. This demonstrates that the dynamic discrete states used in the proposed approach and SWELM-SMEFC are more reasonable and practical than fixed ones in EVIPO-KNN to represent the health of different degrading engine units. In IBL, the number of neighbors used in the k-nearest train instances for RUL estimation is also pre-defined according to the best results.

In terms of in time and late prediction, the proposed approach can achieve the best accuracy with 78 in time prediction and the least late prediction that is only 6 among these approaches. From the aspect of score, the proposed approach is comparable with the LR-ED₂, the Embed-LR₁ and the RULCLIPPER. It should be noted that the best performance with respect to score in RULCLIPPER is obtained by using various combinations of features to choose the best set of features. In terms of other evaluation metrics, the proposed approach achieves the best performance with MSE = 153.7, mean absolute error MAE = 7.34 and MAPE = 9.95% compared to other prognostics approaches. From the above discussions, it is evident that the results obtained in this study is very competitive compared to other prognostics approaches. Generally, it is quite challenging for prognostics to achieve the continuous states of degrading signals when prior experience or information about degradation process is not available. As a matter of fact, in this proposed approach, the degradation of aero-engines can be self-predicted by combining the prediction of continuous states and discrete states simultaneously. Besides, the RUL estimation is achieved with high accuracy and low score. Therefore, the proposed approach is effective for remaining useful life estimation and has a certain impetus on improving the practical applications of prognostics and health management.

V. CONCLUSIONS

In this paper, we propose a novel prognostics approach with self-joint prediction of continuous and discrete states and apply it in the RUL estimation of aero-engines. In the proposed approach, the degradation process is evaluated based on the continuous and discrete states. The continuous states depict the values of degrading signals and the discrete ones represent the fault modes. In our work, the prediction of the degrading signals and the determination of the fault modes are simultaneously achieved based on the QKRLS algorithm. The QKRLS algorithm owns the self-evolving learning capability to evolve its kernel centers according to the data properties. Thus, the discrete states indicated by the kernel centers are decided dynamically according to the self-evolving learning process and can be automatically achieved for different engines which degrade diversely according to their operational conditions and environments. This avoids the pre-assumed fault modes

before hand and improves the RUL estimation accuracy. Within the QKRLS learning framework, the predictors used to predict the future degrading signals are constructed jointly based on the self-evolving learning. This is different from previous approaches in which the predictors and fault modes are decided separately and this further reduces the complexity of the RUL estimation process. As far as we are concerned, the precision of predicting the degrading signals has great effects on the RUL estimation. It requires not only predicting with good performance but also stopping prediction at the right time. Two matching criteria, that is RMSE and distance criteria are adopted to get the optimum predictor and then the RUL is achieved once the predicted degrading signals fall into the final state determined by the optimum predictor. Finally, Turbofan engine datasets from NASA data repository are used to validate the performance of the proposed approach and the results demonstrate the reasonability and superiority of the proposed approach compared to other methods. The accuracy of RUL estimation also depends on the sensors selection. In the future, further study will focus on the investigation of self-evolving feature extraction leading to the best RUL estimation.

VI. ACKNOWLEDGMENTS

This work was supported by the Fundamental Research Funds for the Central Universities, 973 Program (No. 2015CB351703), National Natural Science Foundation of China (No. 91648208). It was also supported in part by the Science and Technology Development Fund of Macao S.A.R (FDCT) under MoST-FDCT Joint Grant 015/2015/AMJ.

REFERENCES

- [1] B. MacIsaac and R. Langton, eds., *Prognostics and health monitoring systems*. Hoboken, NJ, USA: John Wiley & Sons, Ltd, 2011.
- [2] D. L. Iverson, R. Martin, M. Schwabacher, L. Spirkovska, W. Taylor, R. Mackey, J. P. Castle, and V. Baskaran, "General purpose data-driven monitoring for space operations," *Journal of Aerospace Computing Information and Communication*, vol. 9, no. 2, pp. 26–44, 2012.
- [3] D. An, N. H. Kim, and J. H. Choi, "Options for prognostics methods: A review of data-driven and physics-based prognostics," in *54th AIAA/ASME/ASCE/AHS/ASC Structures, Structural Dynamics, and Materials Conference*, (Boston, America), pp. 1–19, 8–11 Apr. 2013.
- [4] A. Saxena and K. Goebel, "Turbofan engine degradation simulation data set," in *NASA Ames Prognostics Data Repository*, NASA Ames Research Center, 2008. <https://ti.arc.nasa.gov/tech/dash/groups/pcoc/prognostic-data-repository/#turbofan>, Accessed 31 Mar. 2018.
- [5] F. O. Heimes and B. Systems, "Recurrent neural networks for remaining useful life estimation," in *2008 International Conference on Prognostics and Health Management*, (Denver, USA), pp. 1–6, 6–9 Oct. 2008.
- [6] R. Khelif, B. Chebel-Morello, S. Malinowski, E. Laajili, F. Fnaiech, and N. Zerhouni, "Direct remaining useful life estimation based on support vector regression," *IEEE Transactions on Industrial Electronics*, vol. 64, no. 3, pp. 2276–2285, 2017.
- [7] G. S. Babu, P. Zhao, and X.-L. Li, "Deep convolutional neural network based regression approach for estimation of remaining useful life," in *International Conference on Database Systems for Advanced Applications*, pp. 214–228, Springer, Cham, 2016.
- [8] R. Khelif, S. Malinowski, B. Chebel-Morello, and N. Zerhouni, "RUL prediction based on a new similarity-instance based approach," in *2014 IEEE 23rd International Symposium on Industrial Electronics (ISIE)*, (Istanbul, Turkey), pp. 2463–2468, 1–4 Jun. 2014.
- [9] E. Ramasso, "Investigating computational geometry for failure prognostics in presence of imprecise health indicator: Results and comparisons on c-mapss datasets," in *European Conference of the Prognostics and Health Management Society 2014*, (Nantes, France), pp. 1–18, 8–10 July. 2014.

- [10] P. Malhotra, V. TV, A. Ramakrishnan, G. Anand, L. Vig, P. Agarwal, and G. Shroff, "Multi-sensor prognostics using an unsupervised health index based on lstm encoder-decoder," in *1st ACM SIGKDD Workshop on Machine Learning for Prognostics and Health Management*, (San Francisco, USA), 13-17 Aug. 2016.
- [11] N. Gugulothu, V. TV, P. Malhotra, L. Vig, P. Agarwal, and G. Shroff, "Predicting remaining useful life using time series embeddings based on recurrent neural networks," *International Journal of Prognostics and Health Management*, vol. 9, no. 1, pp. 1–10, 2018.
- [12] E. Ramasso and R. Gouriveau, "Prognostics in switching systems: Evidential markovian classification of real-time neuro-fuzzy predictions," in *2010 Prognostics and System Health Management Conference*, (Macao, China), pp. 1–10, 12-14 Jan. 2010.
- [13] E. Ramasso, M. Rombaut, and N. Zerhouni, "Joint prediction of continuous and discrete states in time-series based on belief functions," *IEEE Transactions on Cybernetics*, vol. 43, no. 1, pp. 37 – 50, 2013.
- [14] K. Javed, R. Gouriveau, and N. Zerhouni, "Novel failure prognostics approach with dynamic thresholds for machine degradation," in *39th Annual Conference of the IEEE Industrial Electronics Society (IECON)*, (Vienna, Austria), pp. 4404–4409, 10-13 Nov. 2013.
- [15] K. Javed, R. Gouriveau, and N. Zerhouni, "A new multivariate approach for prognostics based on extreme learning machine and fuzzy clustering," *IEEE Transactions on Cybernetics*, vol. 45, no. 12, pp. 2626–2639, 2015.
- [16] B. Chen, S. Zhao, P. Zhu, and J. C. Principe, "Quantized kernel recursive least squares algorithm," *IEEE Transactions on Neural Networks and Learning Systems*, vol. 24, no. 9, pp. 1484 – 1491, 2013.
- [17] H.-J. Rong, N. Sundararajan, G.-B. Huang, and P. Saratchandran, "Sequential adaptive fuzzy inference system (SAFIS) for nonlinear system identification and prediction," *Fuzzy Sets and Systems*, vol. 157, no. 9, pp. 1260–1275, 2006.
- [18] R.-J. Bao, H.-J. Rong, P. Angelov, B. Chen, and P. K. Wong, "Correntropy-based evolving fuzzy neural system," *IEEE Transactions on Fuzzy Systems*, DOI: 10.1109/TFUZZ.2017.2719619, 2017.
- [19] B. Chen, S. Zhao, P. Zhu, and J. C. Principe, "Quantized kernel least mean square algorithm," *IEEE Transactions on Neural Networks and Learning Systems*, vol. 23, no. 1, pp. 22–32, 2012.
- [20] W. Liu, J. C. Principe, and S. Haykin, *Kernel adaptive filtering: a comprehensive introduction*. New York, NY, USA: Wiley, 2010.